

1-1-2010

Imaging spontaneous MMTVneu transgenic murine mammary tumors: targeting metabolic activity versus genetic products.

Mathew L Thakur

Thomas Jefferson University, Madhukar.Thakur@jefferson.edu

Devakumar Devadhas

Thomas Jefferson University


Kaijun Zhang

Thomas Jefferson University, Kaijun.Zhang@jefferson.edu

Richard G Pestell

Thomas Jefferson University, Richard.Pestell@jefferson.edu

Chenguang Wang

*Thomas Jefferson University, Chenguang.Wang@jefferson.edu**See next page for additional authors*[Let us know how access to this document benefits you](#)Follow this and additional works at: <http://jdc.jefferson.edu/radiologyfp> Part of the [Medical Cell Biology Commons](#), [Medical Molecular Biology Commons](#), [Medical Pathology Commons](#), and the [Radiology Commons](#)

Recommended Citation

Thakur, Mathew L; Devadhas, Devakumar; Zhang, Kaijun; Pestell, Richard G; Wang, Chenguang; McCue, Peter; and Wickstrom, Eric, "Imaging spontaneous MMTVneu transgenic murine mammary tumors: targeting metabolic activity versus genetic products." (2010). *Department of Radiology Faculty Papers*. Paper 17.

<http://jdc.jefferson.edu/radiologyfp/17>

Authors

Mathew L Thakur, Devakumar Devadhas, Kaijun Zhang, Richard G Pestell, Chenguang Wang, Peter McCue, and Eric Wickstrom

Imaging Spontaneous MMTVneu Transgenic Murine Mammary Tumors: Targeting Metabolic Activity Versus Genetic Products

Mathew L. Thakur^{1,2}, Devakumar Devadhas¹, Kaijun Zhang¹, Richard G. Pestell², Chenguang Wang², Peter McCue³, and Eric Wickstrom^{2,4}

¹Department of Radiology, Kimmel Cancer Center, Philadelphia, Pennsylvania; ²Department of Cancer Biology, Kimmel Cancer Center, Philadelphia, Pennsylvania; ³Department of Pathology, Anatomy and Cell Biology, Thomas Jefferson University, Philadelphia, Pennsylvania; and ⁴Department of Chemistry and Molecular Biology, Thomas Jefferson University, Philadelphia, Pennsylvania

Despite the great strides made in imaging breast cancer (BC) in humans, the current imaging modalities miss up to 30% of BC, do not distinguish malignant lesions from benign ones, and require histologic examinations for which invasive biopsy must be performed. Annually in the United States, approximately 5.6 million biopsies find benign lesions. More than 50% of human BCs overexpress cyclin D1, and all BCs exhibit VPAC1 oncogene products. Together, these gene products may provide an excellent biomarker for the early and accurate detection of BC. We have evaluated 4 biologically active peptide analogs that have high affinity for VPAC1. The transgenic MMTVneu mice spontaneously develop BC and metastatic lesions that overexpress cyclin D1 and VPAC1 biomarkers. The MMTVneu mouse, therefore, provides an excellent animal model that mimics the pathogenesis of human BC. The objective of this investigation was to determine the ability of 1 of the peptide analogs, ⁶⁴Cu-TP3805, to detect BC in MMTVneu mice using ¹⁸F-FDG as a gold standard. **Methods:** The transgenic MMTVneu mouse colony was maintained. Offspring were screened for transgenic status by reverse transcriptase polymerase chain reaction (RT-PCR). Nine mice with visible, palpable, or unknown metastatic lesions were entered into the protocol. ¹⁸F-FDG (6,475 ± 1,628 kBq [175 ± 44 μCi]) PET served as a control, followed by a CT scan and 24–48 h later by PET with ⁶⁴Cu-TP3805 (4,588 ± 962 kBq [124 ± 26 μCi]). RT-PCR on excised tumors determined VPAC1 expression, and histology ascertained the pathology. **Results:** Ten tumors were detected by PET. Four tumors were detected both by ¹⁸F-FDG and by ⁶⁴Cu-TP3805. Additionally, 4 tumors were imaged with ⁶⁴Cu-TP3805 only. These 8 tumors overexpressed VPAC1 receptors and were malignant by histology. The 2 remaining tumors were visualized with ¹⁸F-FDG only. These tumors did not express the VPAC1 oncogene product and had benign histology. The standard uptake value ranged from 3.1 to 18.3 for ⁶⁴Cu-TP3805 and 0.9 to 1.4 for ¹⁸F-FDG. **Conclusion:** ⁶⁴Cu-TP3805 identified all malignant lesions unequivocally that overexpressed the VPAC1 oncogene surface product. The 2 benign tumors that did not express the VPAC1 re-

ceptor were not imaged. ⁶⁴Cu-TP3805 promises to have the potential for the early and accurate imaging of primary and metastatic BC.

Key Words: oncogenic PET; PET of breast cancer; transgenic MMTVneu mouse model; ⁶⁴Cu-TP3805; oncogenic vs. metabolic imaging

J Nucl Med 2010; 51:106–111

DOI: 10.2967/jnumed.109.069542

Our interest in targeting gene products for the imaging of mammary tumors stems from the fact that mammography, ultrasonography, CT, and MRI miss up to 30% of malignant lesions in the human breast (1–10). Furthermore, any suggestive lesions that are found must be examined by histology, which requires invasive biopsy. An estimated 37 million mammograms were performed in 2007 in the United States. Approximately 7 million (20%) of those mammogram results were abnormal (11). Histologic analyses found benign pathology in 80% of those biopsy samples taken from mammograms with abnormal findings (5.6 million). The challenge has been to develop an imaging agent that will target a specific, fingerprint biomarker that will visualize malignant breast lesions early and reliably.

The oncogene product VPAC1, named for vasoactive intestinal peptide and pituitary adenylate cyclase activating peptide combined, is overexpressed at the onset of oncogenesis. Targeting VPAC1 receptors, therefore, provides an opportunity for the early and accurate imaging of breast cancer. We have performed extensive preclinical molecular imaging studies, both ex vivo and in athymic nude mice bearing human breast cancer xenografts, that offer highly promising results (12,13). In these studies we have targeted VPAC1 receptors that are overexpressed on all breast cancers (14). Approximately 10⁴ VPAC1 receptors are expressed per malignant cell (15,16). Thus far, however, most imaging has been performed using those breast cancers that

Received Aug. 19, 2009; revision accepted Oct. 7, 2009.

For correspondence or reprints contact: Mathew L. Thakur, Laboratories of Radiopharmaceutical Research and Molecular Imaging, Radiology and Radiation Oncology, Thomas Jefferson University, 1020 Locust St., Ste. 359, JAH, Philadelphia, PA 19107.

E-mail: Mathew.Thakur@jefferson.edu

COPYRIGHT © 2010 by the Society of Nuclear Medicine, Inc.

were xenografts, experimentally implanted and physically visible in mice.

Although such tumor imaging is consistent with the practice for preclinical research, an investigation in a model system that will resemble the real, clinical situation would be preferable. Therefore, in this study, we describe an approach that mimics imaging the onset of breast tumors in humans. The *HER2* transgenic mouse model friend virus B-type (FVB)/N-Tg(MMTVneu)202Mul/J overexpresses the murine *HER2* protein driven by a mouse mammary tumor virus (MMTV) promoter (17,18). The female MMTVneu mice develop focal hyperplastic, dysplastic mammary tumors as early as 4 mo, with a median of 7 mo. By 1 y of age, 80% of the female mice display mammary fat-pad tumors (17). Three fourths of the tumors metastasize to the lung at later stages (17). The MMTVneu tumors also overexpress the cyclin D1 gene product protein within the malignant cell and VPAC1 receptor protein on the cell surfaces. These characteristics render the MMTVneu transgenic mouse an ideal target for imaging the onset of breast cancer in a fashion that resembles the pathogenesis of human breast cancer.

We have developed 4 peptide analogs that display high affinity for the VPAC1 receptors (12). The peptides are radiolabeled with ^{64}Cu , a positron-emitting (17.4%) radionuclide with a half-life of 12.7 h (13), via an N_2S_2 chelating diaminedibenzylthio group connected to a lysine residue and separated by a flexible, hydrophilic spacer to avoid steric hindrance (14,19). Biologic activity of the peptide was not compromised by the addition of the chelator. TP3805 has a high affinity for VPAC1 Kd, 3.3×10^{-9} M) and excellent stability in vivo (12). Digital autoradiographic studies showed 6 times greater ^{64}Cu uptake in human BC specimens than in the adjacent normal tissues (12). Furthermore, the uptake in human breast tumors grown in athymic nude mice was high (12).

The purpose of this translational research was to examine the ability of the ^{64}Cu peptide analogs, specifically ^{64}Cu -TP3805, to image spontaneously grown, known and unknown tumors in transgenic MMTVneu mice. ^{18}F -FDG PET served as a gold standard for molecular imaging. Quantitative reverse transcriptase polymerase chain reaction (RT-PCR) on excised tumors was performed to confirm the expression of VPAC1 mRNA. Histology was performed to ascertain tumor pathology.

MATERIALS AND METHODS

MMTVneu Mice

MMTVneu mice of the FVB strain were previously described (18). Offspring were screened by PCR for their genetic status. Twice weekly, animals were examined visually and by gentle palpation for the presence of tumors. Once a tumor was detected, the animals ($n = 9$) were entered into the study within 1–3 wk.

^{18}F -FDG

^{18}F -FDG was obtained commercially from PETNET Solutions, and a dose with predetermined quantity was drawn in a sterile,

1-mL tuberculin syringe. A calibrated ionization chamber, CRC-15 (Capintec), was used for the measurement of radioactivity before and immediately after administration through a lateral tail vein of anesthetized mice. PET was performed 1 h later.

Synthesis and Evaluation of TP3805

The synthesis, purification, and characterization of VPAC1 receptor-specific peptides and their radiolabeling with ^{64}Cu -chloride, including in vivo stability, were described previously (12). The pituitary adenylate cyclase activating peptide (PACAP) analog TP3805 was used in this study. Briefly, the PACAP analog with a C-terminal diaminedithiol (N_2S_2) chelator was synthesized (12,13) on a Wang resin using an ABI 341A peptide synthesizer (Applied Biosystems). Fmoc-Lys (ivDde) was first introduced at the C terminus of the peptide, followed by 4-aminobutyric acid (γ -Aba). The 39-amino-acid-long PACAP sequence was then assembled by standard Fmoc coupling with the final histidyl residue, being a t-Boc-protected His(Trt) derivative. The capping t-Boc function was necessary to ensure that the N-terminal amino group remained protected during subsequent deprotection and coupling cycles performed at the γ -amino group of the C-terminal lysine. The ivDde group at the C-terminal lysine was then selectively removed with 2% hydrazine, followed by the successive additions of di-Fmoc-L-diaminopropionic acid and *S*-benzoylthioglycolic acid. The resulting protected diaminedithiol (NS-benzoyl) $_2$ -containing PACAP peptide was cleaved from the resin using trifluoroacetic acid (TFA):water:phenol:thioanisole/ethanedithiol (82.5:5:5:5:2.5) and precipitated with diethyl ether.

The crude peptide was purified to homogeneity by reversed-phase high performance liquid chromatography (HPLC) (Waters; Millipore) on a Vydac C4 column (5 μm , 10 \times 250 mm). The mass of the analog-chelator construct was confirmed by electrospray mass spectrometry. Following the general synthetic scheme, TP3805 was prepared, purified, and characterized by American Peptide Co.

Preparation of ^{64}Cu -TP-3805 and Quality Control

^{64}Cu (half-life = 12.7 h, β^+ = 17.4%) was obtained once a week either from Washington University, MDS-Nordion, or Trace Laboratories, in 0.1 M HCl. Specific activity (MBq/mL [mCi/mL]) varied from batch to batch and ranged from 1,073 to 37,000 MBq/mL (29–1,000 mCi/mL). The copper content in ^{64}Cu from MDS-Nordion was much greater (1 μg /185 MBq [1 μg /5 mCi]) than that in the ^{64}Cu preparations from Washington University.

Twenty micrograms of each peptide were dispensed in 4 μL of 0.1 M ammonium acetate, pH 6.4, in 5 mL in a clean glass test tube; 100 μg of $\text{SnCl}_2 \cdot 2\text{H}_2\text{O}$ (in 4 μL of 0.1 M HCl) was added as a deprotecting agent, followed by 200 μL of 0.2 M glycine, pH 9.1, to 2 μL of ^{64}Cu in 0.1 M HCl, which was vortexed and heated for 45 min at 90°C. The final pH was approximately 7.5.

Analysis was performed using a Rainin HPLC with a reversed-phase C_{18} Microbond column (Varian Inc.) eluted with a linear 28-min gradient from 10% acetonitrile in 0.1% aqueous TFA to 90% acetonitrile in aqueous 0.1% TFA. A typical HPLC elution profile is shown in Figure 1, which indicates nearly quantitative labeling of a peak at a retention time of 6.7 min. Labeling efficiency was always greater than 95% of total ^{64}Cu . Depending on the initial ^{64}Cu activity, specific activity ranged between 7.4 and 37 Gbq/ μmol (0.2–1.0 Ci/ μmol).

PET/CT

The animal protocol was approved by the Jefferson University Institutional Animal Care and Use Committee. Animals were kept

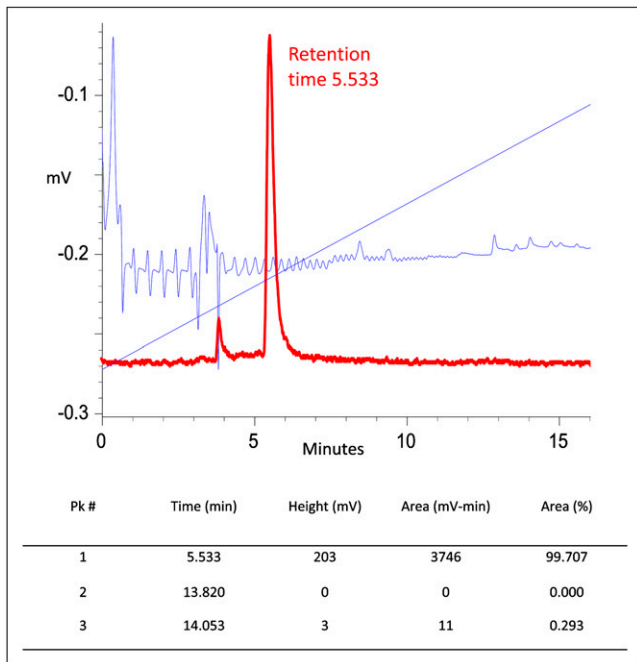


FIGURE 1. HPLC elution profile for ^{64}Cu -TP3805. Radioactivity (99.7%) was eluted in single peak at retention time 5.53 min. Unbound ^{64}Cu elutes at approximately 4 min. Diagonal line is percentage solvent gradient. Blue line indicates peptide ultraviolet elution; peptide mass injected was too small for ultraviolet detection. Pk # = peak number.

fasting for 4 h before the administration of ^{18}F -FDG ($6,475 \pm 1,628$ kBq [175 ± 44 μCi]) via a lateral tail vein. ^{64}Cu -TP3805 ($4,588 \pm 962$ kBq [124 ± 26 μCi]) was administered 24–48 h after the ^{18}F -FDG study. During imaging, animals were anesthetized with an intraperitoneal injection of a mixture of ketamine, xylazine, and acetopromazine. Animals were kept warm and not under anesthesia during the radioactive uptake period. PET was followed by CT, performed at 1 h after the injection of ^{18}F -FDG. When the animals were injected with ^{64}Cu -TP3805, CT was performed first, followed by PET at 4 and 24 h after the injection.

PET was performed using an Inveon microPET scanner (Siemens Medical Solutions), which was known to have the highest spatial resolution (1 mm in full width at half maximum) and sensitivity (>10%) among the commercially available small-animal PET scanners. The highest spatial resolution and sensitivity made the scanner capable of detecting even approximately 0.5-mm-sized lesions, despite low uptake. An ordered-subset expectation maximization 3-dimensional (3D) algorithm with 5 iterations and 8 subsets was used for reconstruction.

CT was performed using a MicroCAT II CT scanner (ImTek Inc.; Siemens), yielding reconstructed voxels of $103 \times 103 \times 103$ μm . A Feldkamp, Davis, and Kress cone-beam algorithm was used for reconstruction. 3D visualization software provided high-quality images including surface-rendered and maximum-intensity-projection images.

Image Processing, Quantification, and Visualization

An Inveon Research Workstation (Siemens) was used for image processing and analysis. An automatic rigid registration algorithm with weighted mutual information as a measure of similarity was

used for registering PET and CT datasets. The anatomic location of the tumor was identified from the registered datasets. Volumes of interest (VOIs) were created on the tumors, and standardized uptake values (SUVs) for body weight were obtained. VOIs were created on the PET images. The PET scanner was calibrated with known activity to get the SUV for body weight values from the VOI. Amira (Visage Imaging Inc.) was used for 3D visualization. PET and CT datasets were registered in Amira using a rigid registration algorithm with normalized mutual information as the measure of similarity. Surface rendering was performed using the threshold pixel value for bone from the CT dataset and the tumor from the PET dataset to localize the tumor with reference to the skeleton. More anatomic structures were rendered from CT when it was not able to localize the tumor with skeleton alone. The anatomic location of the tumor obtained from the visualization was used to excise the tissue from the tumor for histopathology and RT-PCR.

Reverse Transcription and RT-PCR

The goal of RT-PCR was to ascertain that the lesions imaged by ^{64}Cu -TP3805 and by ^{18}F -FDG expressed VPAC1 receptors. The excised tumor tissue architecture was immediately disrupted by the addition of Trizol (Invitrogen Life Technologies) in the presence of 2.3-mm zirconia/silica beads to release the RNA and then homogenized by rapid agitation using the procedure recommended by the manufacturer (BioSpec Products). The RNA was extracted, and the total RNA was then reverse-transcribed using the predeveloped TaqMan assay reagents (Applied Biosystems) for 1 h. The resulting single-strand cDNA was diluted and used as a template for the PCR with TaqMan master mix, using specific primers and probes for VPAC1. RT-PCR was performed

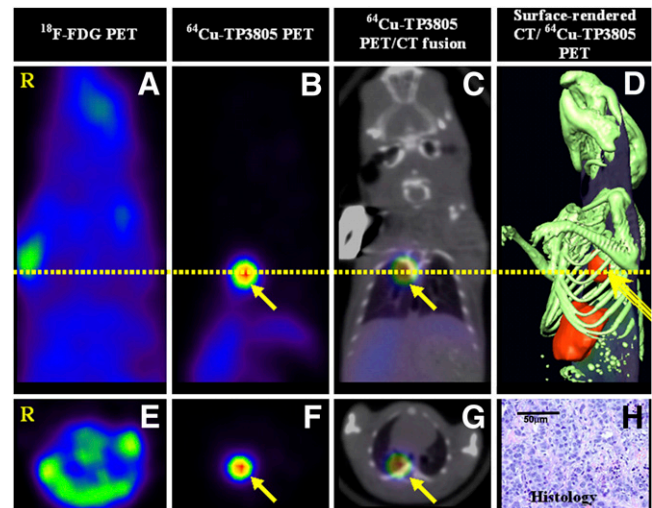


FIGURE 2. (A–C) Coronal PET slices of MMTVneu mouse. (D) Surface-rendered CT/ ^{64}Cu -TP3805 PET image. (E–G) Axial slices through dotted yellow line. (H) Tumor histology. Spontaneously grown, unpalpable, and invisible tumor in intact MMTV mouse was unequivocally detectable by ^{64}Cu -TP3805 (B, yellow arrow) but not by ^{18}F -FDG (A). Fusion and surface-rendered ^{64}Cu -TP3805 images (C and D) depict that it was lung metastatic lesion. RT-PCR demonstrated VPAC1 oncogene product expression, and histology (H) showed malignant status of tumor (Rs in leftmost panels indicate right of mouse).

using a CFD-3200 DNA Engine Opticon System (Bio-Rad Laboratories) and the following cycling conditions: 95°C for 15 s and 60°C for 1 min for 50 cycles. The expression levels of the VPAC1 mRNA were determined from the cycle threshold (C_T) values normalized to human glyceraldehyde-phosphate dehydrogenase and standard curves used for calculation (20).

Histology

Immediately after PET, animals were sacrificed by CO₂ inhalation. Tumors were excised and then placed in 10% formaldehyde in phosphate-buffered saline. These were then embedded in paraffin blocks by the institutional histology core facility. Histologic slides (10 μm thick) were prepared and stained with hematoxylin and eosin. The slides were then read by an attending pathologist.

RESULTS

The radiochemical purity of ⁶⁴Cu-TP3805, as determined by HPLC, is shown in Figure 1 and was consistent with all preparations used. The specific activity of these preparations ranged between 7.4 and 37 Gbq/μmol (0.2 and 1.0 Ci/μmol). In 9 mice studied, a total of 10 tumors were identified by both probes, ¹⁸F-FDG and ⁶⁴Cu-TP3805. Of these, 4 were visualized, each with ⁶⁴Cu-TP3805 and ¹⁸F-FDG. An additional 4 tumors were visualized with

⁶⁴Cu-TP3805 only (Figs. 2 and 3). The 2 remaining tumors were depicted with ¹⁸F-FDG (Fig. 4) only.

Histology and RT-PCR showed (Fig. 5) that all 8 tumors detected by ⁶⁴Cu-TP3805 were malignant by histology and expressed VPAC1 receptors in severalfold greater quantity than did the normal tissue.

The 2 tumors that were not detectable by ⁶⁴Cu-TP3805 (Fig. 6) but were visualized with ¹⁸F-FDG had benign histology and did not express VPAC1 receptors in any greater quantity than did the normal tissue. One benign mass not detectable by ⁶⁴Cu-TP3805 (Fig. 6) was a cystadenoma of ductal origin. The SUVs for these 8 malignant tumors ranged from 3.1 to 18.3 for ⁶⁴Cu-TP3805 and 0.9 to 1.4 for ¹⁸F-FDG (6 tumors).

DISCUSSION

An estimated 37 million mammograms are obtained annually in the United States (11). Of these, approximately 20% are found to be abnormal and require biopsy for histologic confirmation of this abnormality. Statistical data suggest that approximately 80% (5.6 million) of these histologic examinations find benign pathology. None of the current imaging modalities distinguishes benign lesions

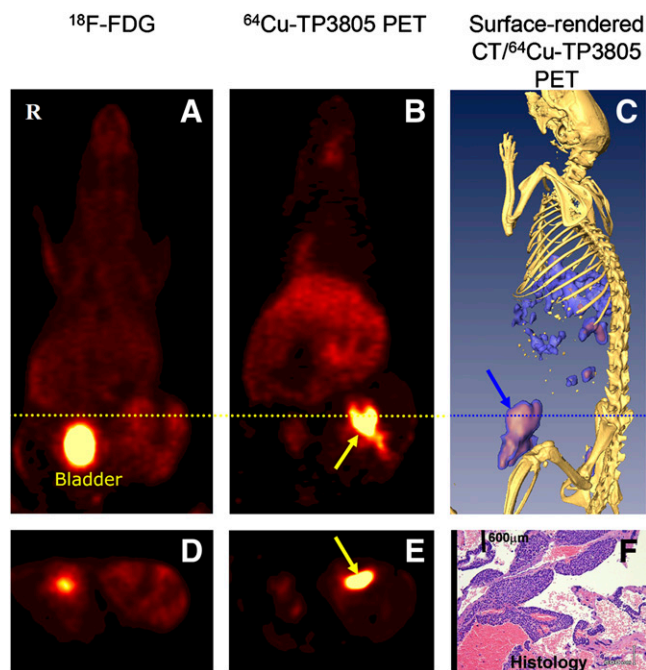


FIGURE 3. (A and B) Coronal PET slices of MMTVneu mouse. (C) Surface-rendered CT/⁶⁴Cu-TP3805 PET image. Visible large primary tumor (yellow arrow) near lowest left nipple had intense ⁶⁴Cu-TP3805 uptake in center of tumor (B). ¹⁸F-FDG uptake (A) in tumor was only faint (SUV, 1; high ¹⁸F-FDG uptake is in bladder). Surface-rendered image (C) depicts anatomic location of tumor (blue arrow). RT-PCR showed VPAC1 expression. Histology (F) showed malignant tumor and surrounding necrotic tissue. (D and E) Axial slices through dotted line.

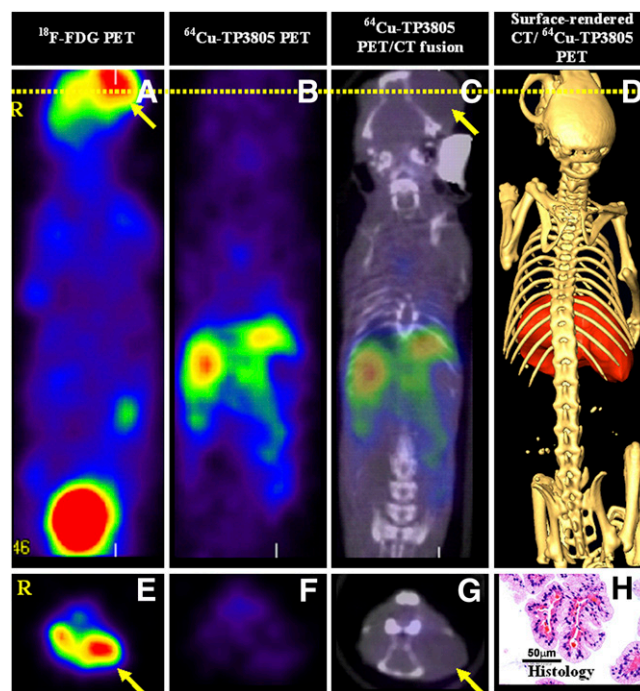


FIGURE 4. (A–C) Coronal PET slices of MMTVneu mouse. (D) Surface-rendered CT/⁶⁴Cu-TP3805 PET image. MMTV mouse had large visible mass in left eye. There was intense ¹⁸F-FDG uptake in lesion (A, yellow arrow) (R represents animal's right; lower red spot is ¹⁸F-FDG uptake in bladder). There was no ⁶⁴Cu-TP3805 uptake in lesion (B–D) except in liver and spleen (B and C). RT-PCR showed no over-expression of VPAC1. Histology (lower right, H) showed lesion was benign cystadenoma of ductal origin. (E–G) Axial slices through dotted yellow line.

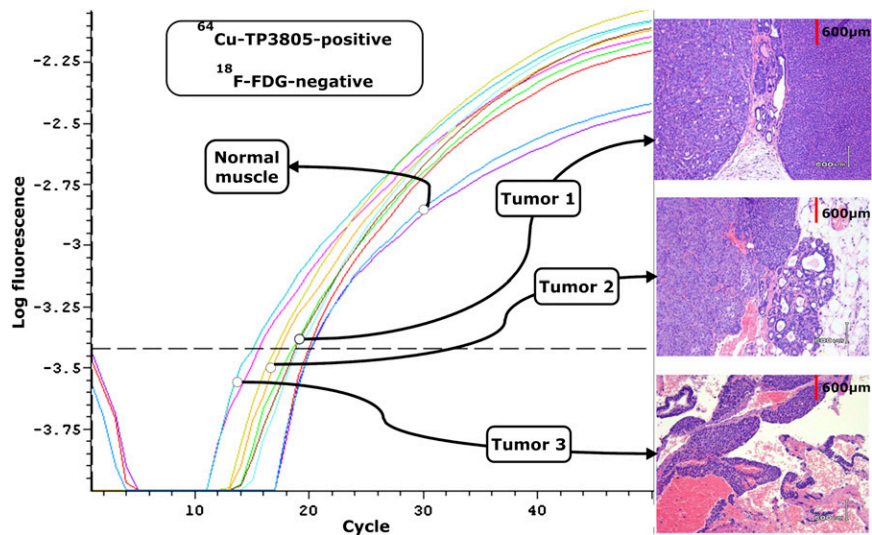


FIGURE 5. Composite of RT-PCR curves and histology of 3 tumors from 3 separate MMTV mice. All 3 tumors had intense ^{64}Cu -TP3805 uptake. RT-PCR showed overexpression of VPAC1 receptors, compared with normal tissue, and histology revealed that tumors were malignant. However, ^{18}F -FDG images were normal for all 3 tumors.

from malignant tumors. Furthermore, they miss up to 30% of breast tumors (1–10). A compelling need exists for a probe that will detect breast cancer early and accurately. Such a probe could also minimize the need for invasive biopsy in the future. In turn, a reliable molecular probe could improve the management of breast cancer, minimize the number of biopsies, reduce patient trauma, and save significantly on health-care costs.

An array of new radiopharmaceuticals, contrast agents, and hybrid equipment is being prepared and investigated to accomplish this goal. We hypothesized that the VPAC1 oncogene product (which is overexpressed on 100% of breast cancer cells, regardless of their hormonal status at the onset of oncogenesis) will serve as a specific biomarker for the early and accurate detection of breast cancers. Our probe, TP3805, is an analog of PACAP (12) and has a high receptor specificity and high affinity for VPAC1. TP3805 is stable in vivo and when injected in nanomolar to micromolar quantities does not induce any adverse effects (Zhang et al., unpublished data, 2008).

The data presented here demonstrate the ability of TP3805 to detect known and unknown tumors, grown spontaneously, that mimic human breast cancer pathophysiology. The data also show that TP3805 has the unique characteristic derived by its biomarker specificity of distinguishing benign lesions from malignant tumors. If this ability of ^{64}Cu -TP3805 prevails in human subjects, then in the future, PET with ^{64}Cu -TP3805 will significantly affect the management of breast cancer. Cancer is the disease of molecular cell biology. VPAC1 receptors are overexpressed at the onset of BC; specifically targeting VPAC1 receptors provides the early detection of primary and metastatic lesions (21). However, only human clinical data will verify the merits and the limitations of ^{64}Cu -TP3805 in the management of patients with well-differentiated BC, metastatic lesions, and ductal carcinoma in situ.

^{18}F -FDG, the most commonly used radiopharmaceutical in oncologic PET, is a nonspecific agent that reflects on the metabolic activity of a lesion. It does not have the ability to identify or characterize lesions by their genomic nature or

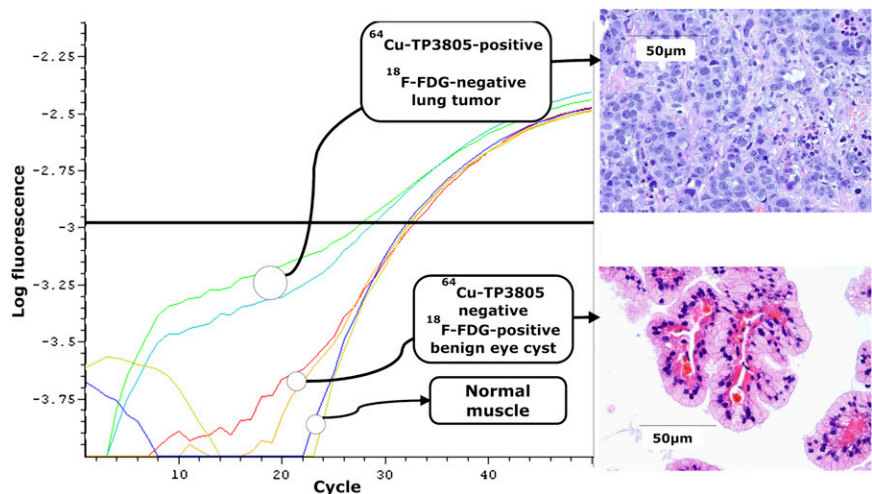


FIGURE 6. Composite of RT-PCR curves and histology of 2 tumors from 2 separate MMTV mice. Upper panel shows 1 tumor with malignant histology that overexpressed VPAC1 oncogene product. This tumor had intense ^{64}Cu -TP3805 uptake but no abnormal ^{18}F -FDG uptake. Tumor in lower panel was the in eye of MMTV mouse (shown in Fig. 4). Histology showed it was cystadenoma of ductal origin and did not express VPAC1. There was no uptake of ^{64}Cu -TP3805 in lesion but ^{18}F -FDG uptake was highly abnormal (Fig. 4).

to target specific biomarkers, expressed as a result of oncogenesis. This limits the ability of ^{18}F -FDG to distinguish benign lesions from malignant ones and also to identify lesions, even those that are malignant in pathology. Its specificity for detecting primary BC lesions is only approximately 70% (9,10) and for metastatic BC lesions is only approximately 80% (22,23). These characteristics of ^{18}F -FDG are evidenced in this study in which ^{18}F -FDG missed 4 of 8 malignant tumors and imaged 2 of 2 benign lesions. None of the other imaging modalities, such as mammography, ultrasonography, CT, or MRI, has been shown to stratify benign lesions from malignant ones also. The need for a molecular imaging probe that will address these serious issues is compelling (13,24).

CONCLUSION

On the basis of the data presented in this report and those published previously (12), it is reasonable to conclude that ^{64}Cu -TP3805 has the ability to identify malignant lesions accurately, eliminate those benign masses that do not express the specific biomarkers of breast cancer, and likely contribute to the management of patients with breast cancer.

ACKNOWLEDGMENT

This research was supported by NIH CA-RO1-109231, EB-RO1-001809, RP-RO1-023709, CA- S10RR 023709, PA ME 03184, NuView Inc., and P30 CA56036.

REFERENCES

1. Tse GM, Yang W. Sonographic, mammographic, and histopathologic correlation of symptomatic ductal carcinoma in situ. *AJR*. 2004;182:101–110.
2. Uematsu T, Sano M, Homma K. False-positive helical CT findings of multifocal and multicentric breast cancer: is attenuation of tumor useful for diagnosing enhanced lesions? *Breast Cancer*. 2002;9:62–68.
3. Schnall M, Orel S. Breast MR imaging in the diagnostic setting. *Magn Reson Imaging Clin N Am*. 2006;14:329–337.
4. Ghai S, Muradali D, Bukhanov K, et al. Nonehancing breast malignancies on MRI: sonographic and pathologic correlation. *AJR*. 2005;185:481–487.
5. Smith AP, Hall PA, Marcello DM. Emerging technologies in breast cancer detection. *Radiol Manage*. 2004;26:16–24.
6. Elmore JG, Armstrong K, Lehman CD, et al. Screening for breast cancer. *JAMA*. 2005;293:1245–1256.
7. Berg WA, Gutierrez L, Ness-Aiver MS, et al. Diagnostic accuracy of mammography, clinical examination, US, and MR imaging in preoperative assessment of breast cancer. *Radiology*. 2004;233:830–849.
8. Chagpar A, Middleton L, Sahin AA, et al. Accuracy of physical examination, ultrasonography, and mammography in predicting residual pathologic tumor size in patients treated with neoadjuvant chemotherapy. *Ann Surg*. 2006;243:257–264.
9. Bombardiere E, Crippa F, Baio SM, et al. Nuclear medicine advances in breast cancer imaging. *Tumori*. 2003;87:277–287.
10. Ruibal A, Maldonado A, Sanchez Salmon A, et al. ^{18}F -FDG-PET in patients with situ breast carcinomas: a cause of false negative results [in Spanish]. *Med Clin (Barc)*. 2008;130:332–333.
11. Elter M, Schulz-Wendland R, Wittenberg J. The prediction of breast cancer biopsy outcomes using two CAD approaches that both emphasize an intelligible decision process. *Med Phys*. 2007;34:4164–4172.
12. Zhang K, Aruva M, Shanthly N, et al. Vasoactive intestinal peptide (VIP) and pituitary adenylate cyclase activating peptide (PACAP) receptor specific peptide analogues for PET imaging of breast cancer; In vitro/in vivo evaluation. *Regul Pept*. 2007;144:91–100.
13. Thakur ML. Genomic biomarkers for molecular imaging: predicting the future. *Semin Nucl Med*. 2009;39:236–246.
14. Reubi JC, Laderach U, Waser B, et al. Vasoactive intestinal peptide/pituitary adenylate cyclase-activating peptide receptor subtypes in human tumors and their tissues of origin. *Cancer Res*. 2000;60:3105–3112.
15. Zia H, Hida T, Jakowlew S, et al. Breast cancer growth is inhibited by vasoactive intestinal peptide (VIP) hybrid, a synthetic VIP receptor antagonist. *Cancer Res*. 1996;56:3486–3489.
16. Leyton J, Gozes Y, Zia F, et al. PACAP (6-38) is a PACAP receptor antagonist for breast cancer cells. *Breast Cancer Res Treat*. 1999;56:177–186.
17. Muller WJ, Arteaga CL, Muthuswamy SK, et al. Synergistic interaction of the neu proto-oncogene product and transforming growth factor alpha in the mammary epithelium of transgenic mice. *Mol Cell Biol*. 1996;16:5726–5736.
18. Hulit J, Lee RJ, Li Z, et al. $p27^{Kip1}$ repression of ErbB2-induced mammary tumor growth in transgenic mice involves Skp2 and Wnt/ β -catenin signaling. *Cancer Res*. 2006;66:8529–8541.
19. Pallela VR, Thakur ML, Chakder S, et al. Tc-99m labeled vasoactive intestinal peptide receptor agonist: functional studies. *J Nucl Med*. 1999;40:352–360.
20. Kawakami M, Kimura T, Kishimoto Y, et al. Preferential expression of the vasoactive intestinal peptide (VIP) receptor in human cord blood-derived CD34⁺CD38⁻ cells: possible role of VIP as a growth-promoting factor for hematopoietic stem/progenitor cells. *Leukemia*. 2004;18:912–921.
21. Reubi JC. In vitro identification of VIP receptors in human tumors: potential clinical implications. *Ann NY Acad Sci*. 1996;805:753–759.
22. Isasi CR, Moadel RM, Blaufox DM. A meta-analysis of FDG-PET for the evaluation of breast cancer recurrence and metastases. *Breast Cancer Res Treat*. 2005;90:105–112.
23. Dose-Schwarz J, Mahner S, Schirmacher S, et al. Detection of metastases in breast cancer patients: comparison of FDG PET with chest x-ray, bone scintigraphy and ultrasound of the abdomen. *Nuklearmedizin*. 2008;47:97–103.
24. Thakur ML, Aruva M, Garippa R, et al. PET imaging of oncogene overexpression using Cu-64-VIP analog: comparison with Tc-99m-VIP analog. *J Nucl Med*. 2004;45:1381–1389.